16. "Ice chemistry in starless molecular cores"
J. Kalv̄ans
    Accepted by ApJ
    http://arxiv.org/pdf/1504.06065

17. "A Ring of C2H in the Molecular Disk Orbiting TW Hya"
Joel H. Kastner, Chunhua Qi, Uma Gorti, Pierre Hily-Blant, Karin Oberg, Thierry Forveille, Sean Andrews, David Wilner
    Accepted by ApJ
    http://arxiv.org/pdf/1504.05980

18. "Formation of Super-Earth Mass Planets at 125–250 AU from a Solar-type Star"
Scott J. Kenyon and Benjamin C. Bromley
    Accepted by Astrophysical Journal
    http://arxiv.org/pdf/1501.05659

19. "Evidence for Decay of Turbulence by MHD Shocks in Molecular Clouds via CO Emission"
Rebecca L. Larson, Neal J. Evans II, Joel D. Green, and Yao-Lun Yang
    Accepted by The Astrophysical Journal
    http://arxiv.org/pdf/1505.00847

20. "Smoothed particle magnetohydrodynamic simulations of protostellar outflows with mis- aligned magnetic field and rotation axes"
Benjamin T. Lewis, Matthew R. Bate, and Daniel J. Price
    Accepted by MNRAS
    http://arxiv.org/pdf/1504.08322v1

16. "Ice chemistry in starless molecular cores"
J. Kalv̄ans

ABSTRACT

Starless molecular cores are natural laboratories for interstellar molecular chemistry research. The chemistry of ices in such objects was investigated with a three-phase (gas, surface, and mantle) model. We considered the center part of five starless cores, with their physical conditions derived from observations. The ice chemistry of oxygen, nitrogen, sulfur, and complex organic molecules (COMs) was analyzed. We found that an ice-depth dimension, measured, e.g., in monolayers, is essential for modeling of chemistry in interstellar ices. Particularly, the H_2O:CO:CO_2:N_2:NH_3 ice abundance ratio regulates the production and destruction of minor species. It is suggested that photodesorption during core collapse period is responsible for high abundance of interstellar H_2O_2 and O_2H, and other species synthesized on the surface. The calculated abundances of COMs in ice were compared to observed gas-phase values. Smaller activation barriers for CO and H_2CO hydrogenation may help explain the production of a number of COMs. The observed abundance of methyl formate $HCOOCH_3$ could be reproduced with a 1kyr, 20K temperature spike. Possible desorption mechanisms, relevant for COMs, are gas turbulence (ice exposure to interstellar photons) or a weak shock within the cloud core (grain collisions). To reproduce the observed COM abundances with the present 0D model, 1-10% of ice mass needs to be sublimated. We estimate that the lifetime for starless cores likely does not exceed 1Myr. Taurus cores are likely to be younger than their counterparts in most other clouds.

Subject headings: astrochemistry — molecular processes — ISM: clouds — ISM: abundances — ISM: individual objects (CB 17, CB 26, CB 27, B 68)

>固相上での化学進化の計算

>５つのStarless core　（CB17S, CB17L, CB26, CB27, B68）の中心での観測値

>固相化学を原子種 (O, N, S, complex organic molecules[COM])で解析

>固相の層構造が、星間固体での化学反応のモデリングの本質である

ー固相上の化学反応には特に複層構造[(sub)layer]に強い依存性がある

ー単層での計算は、星間固体での表面化学反応を再現するには不十分である（特に
　minor speciesでは）

ー特にH2O:CO:CO2: N2:NH3の固体の存在量比は、minor speciesの生成と破壊を調整

ーコアの収縮期の光乖離はH2O2,O2H,他の分子種の高い存在量比の原因であると示唆される。

ー固相上のCOMsの計算された存在量は気相上の観測された値と比較した。

ーCOとH2COの水素生成(Hydrogeneration)の低い励起エネルギーは、おそらく多くのCOMsの生成を説明する助けになる。

ーHCOOCH3の観測された存在量は、1kyr, 20Kのspikeで再現できる。

ー考えられるCOMsの破壊のメカニズムは、ガスの乱流や弱いショックである。

ーH2O:CO固体の存在量比で年齢を推定するには危険である。
　　　ーCOはダストの外側の層にあることが多く、気相や他の分子種に容易に変化する
　　　　interstellar photonsやlow-velocity shockによる mild heating によって

>観測されたCOMsの存在量を0D modelで再現し、1-10%の固体質量が昇華する必要がある。

ーO2とH2O2がOの主なreservoirs (H2OやCO2を除いて)であることを見つけた

ーstar less core の存在期間(lifetime)は1Myrを超えないと推定した

＞Taurusは他の分子雲に対して若そうである
　　ーCO2:H2O固体存在比が低い。（44%かそれ以下）
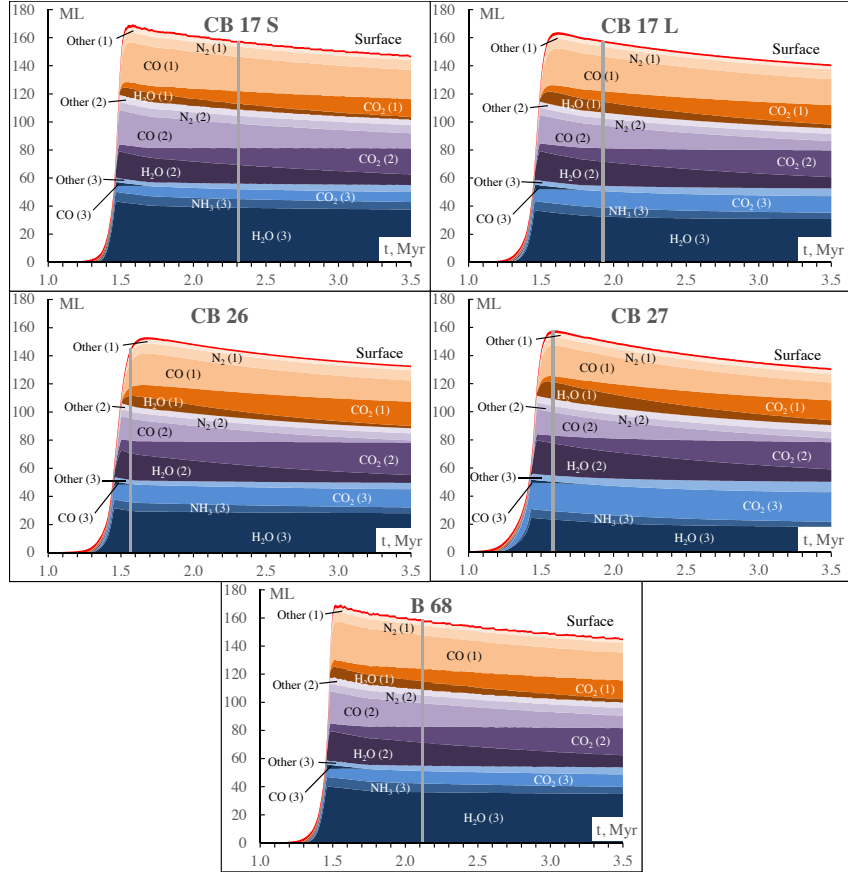　　ー既存のモデルでは650kyr (CB17S core)という値が出るが
　　　　<1Myrということだと考えられる

Fig. 2.— Calculated ice thickness and abundance in MLs for major species in the sublayers for the modeled cloud cores. The number in parenthesis indicates the number of the respective sublayer, while 'Other' stands for all other icy species in that sublayer. The vertical gray line indicates t_{50} for each model.

Table 1: The constant physical parameters of modeled starless cores during their stable Phase 2.

Core	Observational data						Calculated data		
	$n_{H,0}$, cm^{-3}	r_0, AU	r_1, AU	η	N_{out}, cm^{-2}	Ref.	A_V, mag	T, K	t_1, kyr
CB 17 S - SMM1	2.3E+5	9.5E+3	3.0E+4	4.9	0	S[a]	13.8	8.2	1465
CB 17 L - SMM	1.3E+5	1.1E+4	3.0E+4	5.0	3.6E+20	L[b]	9.1	9.2	1451
CB 26 - SMM	8.7E+4	8.0E+3	4.0E+4	3.0	2.2E+20	L	6.5	11.1	1437
CB 27 - SMM	1.3E+5	1.3E+4	6.6E+4	6.0	3.1E+20	L	9.5	8.9	1451
B 68 - SMM	4.0E+5	7.0E+3	2.7E+4	5.0	3.0E+20	L	17.6	7.9	1482

NOTE.—Assumed physical parameters: $n_{H,0}$–density at the center of the core; r_0–radius of the central density plateau; η–power-law slope for density; r_1–radius of the region (core) in consideration; N_{out}–column density of the surrounding cloud. Calculated parameter t_1 is the length of the cloud core collapse Phase 1.

[a]Schmalzl et al. (2014)

[b]Lippok et al. (2013)

Table 4: Changes in reactions respective to the original network by Laas et al. (2011).

No.	New gas phase reactions[a]	α	β	γ	Reference
1	$CH_2OH + H \longrightarrow CH_3 + OH$	1.6E-10	0	0	NIST
2	$CH_2OH + O \longrightarrow H_2CO + OH$	1.5E-10	0	0	NIST
3	$CH_2OH + CH_3 \longrightarrow H_2CO + CH_4$	1.4E-10	0	0	NIST
4	$CH_2OH + CH_3 \longrightarrow C_2H_5OH$	1.0E-15	-3.00	0	Vasyunin & Herbst (2013b)[b]

No.	New surface (ice) reactions	E_A, K			Reference
5	$H + HCO \longrightarrow CO + H_2$	0			This work
6	$OH + HCO \longrightarrow CO + H_2O$	0			This work
7	$NH_2 + HCO \longrightarrow CO + NH_3$	0			This work
8	$H_2 + HCO \longrightarrow CH_3O$	2100[c]			This work
9	$OH + SO \longrightarrow SO_2 + H$	0			Gas phase
10	$O + HS \longrightarrow S + OH$	956			Gas phase
11	$O + HS \longrightarrow SO + H$	0			Gas phase
12	$H + CL \longrightarrow HCL$	0			Gas phase

No.	Changed surface (ice) reactions	E_A, K			Reference
13	$CO + O \longrightarrow CO_2$	290			Roser et al. (2001)
14	$O_2 + H \longrightarrow O_2H$	600			Du et al. (2012)
15	$H + H_2CO \longrightarrow CH_3O$	2100			Woon (2002)
16	$O_3 + H \longrightarrow O_2 + OH$	0			Mokrane et al. (2009)

[a]In addition to the four reactions from Vasyunin & Herbst (2013b). Reaction rate coefficient $k = \alpha(T/300)^\beta \exp(-\gamma/T)$
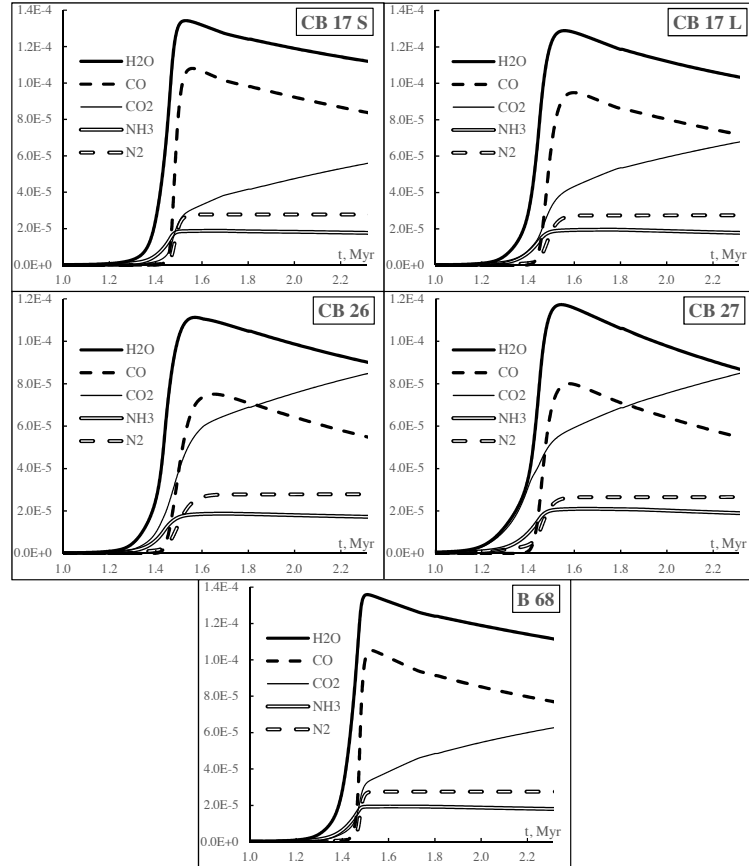[b]Data adopted from $CH_3O + CH_3$ reaction
[c]Estimate

Fig. 3.— Calculated abundances, relative to H atom number density, of major species in ice for the five modeled cores.

17. "A Ring of C2H in the Molecular Disk Orbiting TW Hya"

Joel H. Kastner, Chunhua Qi, Uma Gorti, Pierre Hily-Blant, Karin Oberg, Thierry Forveille, Sean Andrews, David Wilner

ABSTRACT

We have used the Submillimeter Array to image, at $\sim 1.5''$ resolution, C_2H $N = 3 \to 2$ emission from the circumstellar disk orbiting the nearby ($D = 54$ pc), ~ 8 Myr-old, $\sim 0.8\ M_\odot$ classical T Tauri star TW Hya. The SMA imaging reveals that the C_2H emission exhibits a ring-like morphology. Based on a model in which the C_2H column density follows a truncated radial power-law distribution, we find that the inner edge of the ring lies at ~ 45 AU, and that the ring extends to at least ~ 120 AU. Comparison with previous (single-dish) observations of C_2H $N = 4 \to 3$ emission indicates that the C_2H molecules are subthermally excited and, hence, that the emission arises from the relatively warm ($T \stackrel{>}{\sim} 40$ K), tenuous ($n << 10^7\ cm^{-3}$) upper atmosphere of the disk. Based on these results and comparisons of the SMA C_2H map with previous submm and scattered-light imaging, we propose that the C_2H emission most likely traces particularly efficient photo-destruction of small grains and/or photodesorption and photodissociation of hydrocarbons derived from grain ice mantles in the surface layers of the outer disk. The presence of a C_2H ring in the TW Hya disk hence likely serves as a marker of dust grain processing and radial and vertical grain size segregation within the disk.

・SMAでTW HyaをC2H(N=3-2)で観測した

・C2Hで45AU-120AUのリング受かった

　ー45auというのはCO snow line(30au)とsubmm-sizedのダストが急激に弱くなる60au の中間である

・過去のC2H(4-3)の単一境の観測と比較しC2Hはsubthermally excitedである

・相対的に温度が高く(T>40)希薄である(n<<10^7 cm^-3)

・C2Hは小さなダストの光破壊(photo-destruction)が部分的に起きているところ かつ/または炭水化物(hydrocarbon)の光脱離(photodesorption)と光乖離(photodissociation) をトレースしていると考えられる

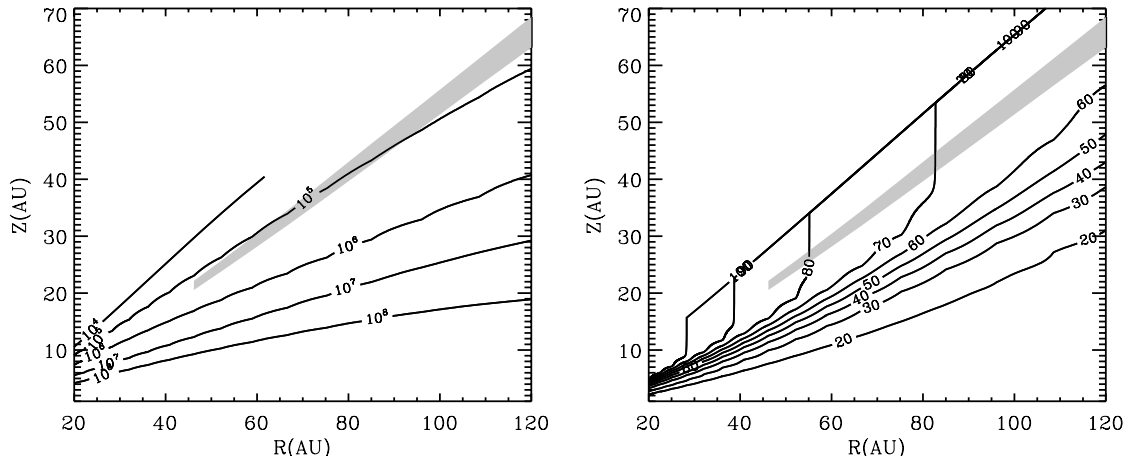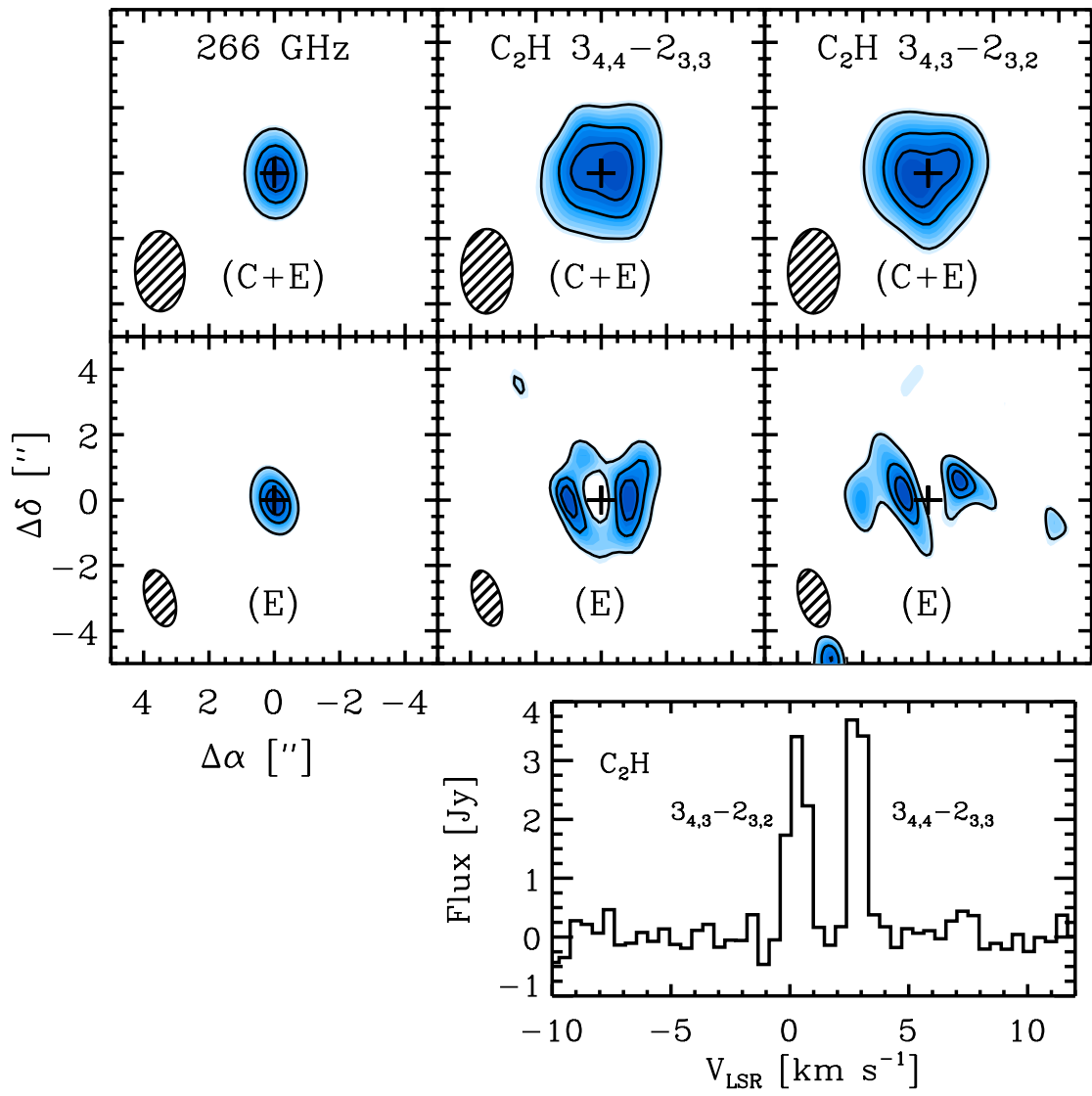・C2Hのリングの存在はダストの過程(processing)や、垂直方向や動径方向のチリのサイ ズの分離のマーカーとして見ることが出来る

Fig. 4.— Distribution of C_2H for the best-fit model, overlaid as grey shading on contour plots of disk density (*left*, in cm^{-3}) and gas kinetic temperature (*right*, in K).

18. "Formation of Super-Earth Mass Planets at 125–250 AU from a Solar-type Star"
Scott J. Kenyon and Benjamin C. Bromley

ABSTRACT

We investigate pathways for the formation of icy super-Earth mass planets orbiting at 125–250 AU around a 1 $M_\odot$ star. An extensive suite of coagulation calculations demonstrates that swarms of 1 cm to 10 m planetesimals can form super-Earth mass planets on time scales of 1–3 Gyr. Collisional damping of $10^{-2}-10^2$ cm particles during oligarchic growth is a highlight of these simulations. In some situations, damping initiates a second runaway growth phase where 1000–3000 km protoplanets grow to super-Earth sizes. Our results establish the initial conditions and physical processes required for *in situ* formation of super-Earth planets at large distances from the host star. For nearby dusty disks in HD 107146, HD 202628, and HD 207129, ongoing super-Earth formation at 80–150 AU could produce gaps and other structures in the debris. In the solar system, forming a putative planet X at $a \lesssim 300$ AU ($a \gtrsim 1000$ AU) requires a modest (very massive) protosolar nebula.

Subject headings: planetary systems – planets and satellites: formation – solar system: formation

・1Msun周りの125au-250auの軌道で氷のスーパーアースの形成経路を調べる

・凝固の計算の広いsuiteは、1cm-10mの微惑星群がsuper-earth massの惑星を1-3Gyrで形成できることを示した。

・寡専成長期の10^-2 ..10^2 cmの粒子の衝突減衰が、これらシミュレーションの重要な点である。

・いくつかの状況で、減衰は、1000-3000km原始惑星からsuper-earth sizeへの第二期急速成長段階を始める

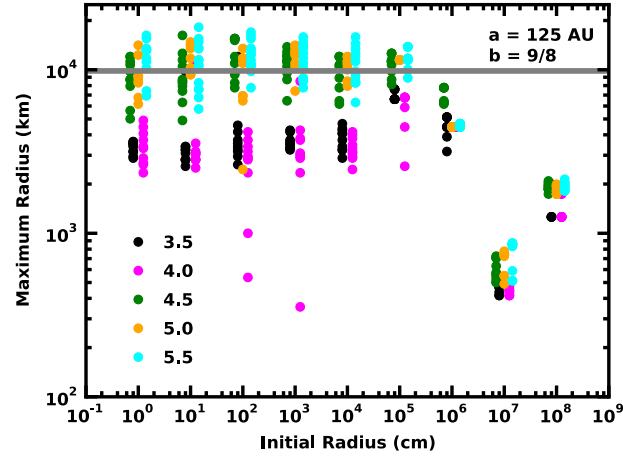・我々の結果は、中心星から大きくはなれた場所でsuper-earth惑星が形成した本来の位置を、初期状態と物理過程を確立した
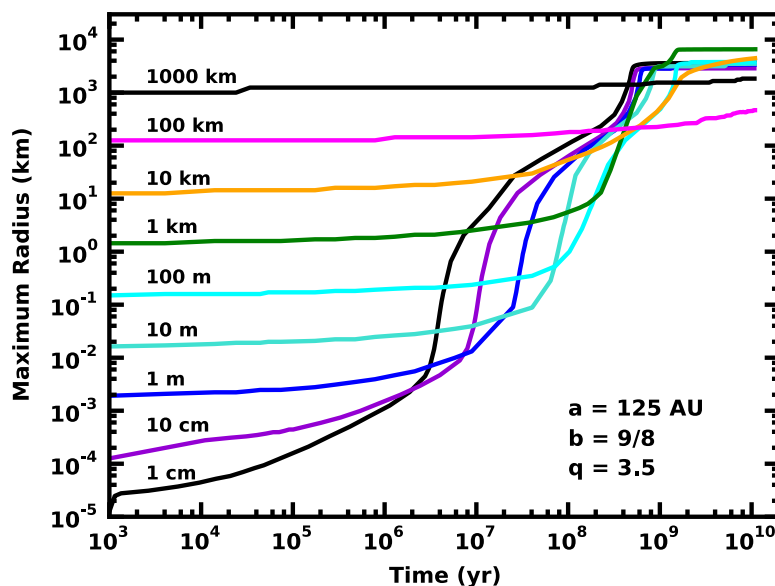
Fig. 4.— Maximum planet radius at $a = 125$ AU as a function of r_0 and q for $b = 9/8$. To improve clarity, points are slightly offset from the nominal r_0. The horizontal grey bar indicates the radius of an Earth-mass planet with $\rho_s = 1.5$ g cm^{-3}. Calculations with $r_0 = 1$ cm to 1 km and $q \gtrsim 4.5$ produce super-Earth mass planets.
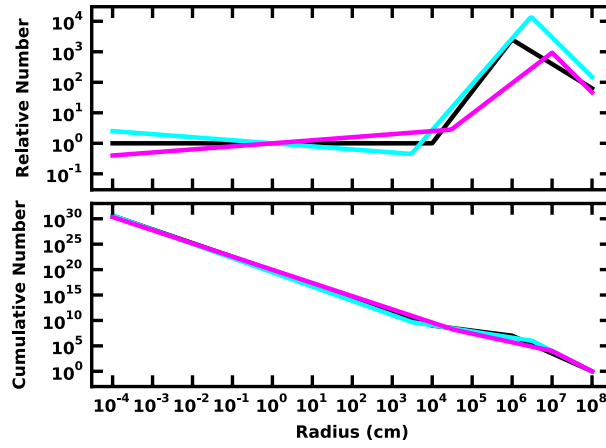

Fig. 6.— Comparison of cumulative (lower panel) and relative cumulative (upper panel) size distributions for three idealized power law size distributions. To construct the relative size distribution, we adopt a normalization with $q_s = 2.7$ which yields $n_{c,rel} \equiv 1$ at $r = 1$ cm. *Black curves:* $n_l = 1$, $q_s = 2.7$, $q_i = 1.0$, $q_l = 3.5$, $r_1 = 0.1$ km, $r_2 = 10$ km. *Cyan curves:* $n_l = 1$, $q_s = 2.8$, $q_i = 1.2$, $q_l = 4.0$, $r_1 = 0.03$ km, $r_2 = 30$ km. *Magenta curves:* $n_l = 1$, $q_s = 2.6$, $q_i = 1.7$, $q_l = 4.0$. $r_1 = 0.3$ km, $r_2 = 100$ km. Relative size distributions allow an easier assessment of the differences between power-law components.

19. "Evidence for Decay of Turbulence by MHD Shocks in Molecular Clouds via CO Emission"

Rebecca L. Larson, Neal J. Evans II, Joel D. Green, and Yao-Lun Yang
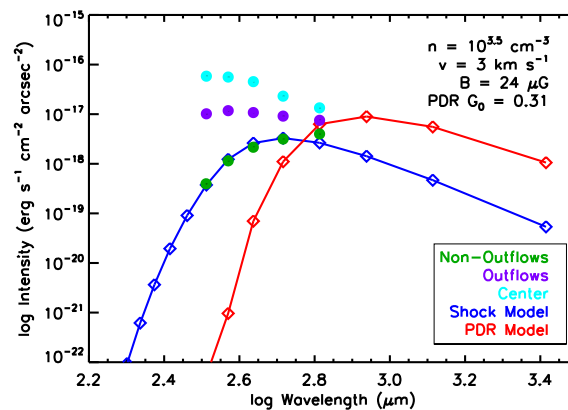
ABSTRACT

We utilize observations of sub-millimeter rotational transitions of CO from a *Herschel* Cycle 2 open time program ("COPS", PI: J. Green) to identify previously predicted turbulent dissipation by magnetohydrodynamic (MHD) shocks in molecular clouds. We find evidence of the shocks expected for dissipation of MHD turbulence in material not associated with any protostar. Two models fit about equally well: model 1 has a density of 10^3 cm^{-3}, a shock velocity of 3 km s^{-1}, and a magnetic field strength of 4 μG; model 2 has a density of $10^{3.5}$ cm^{-3}, a shock velocity of 2 km s^{-1}, and a magnetic field strength of 8 μG. Timescales for decay of turbulence in this region are comparable to crossing times. Transitions of CO up to J of 8, observed close to active sites of star formation, but not within outflows, can trace turbulent dissipation of shocks stirred by formation processes. Although the transitions are difficult to detect at individual positions, our *Herschel*-SPIRE survey of protostars provides a grid of spatially-distributed spectra within molecular clouds. We averaged all spatial positions away from known outflows near seven protostars. We find significant agreement with predictions of models of turbulent dissipation in slightly denser ($10^{3.5}$ cm^{-3}) material with a stronger magnetic field (24 μG) than in the general molecular cloud.

・分子雲内でMHDショックによって乱流が散逸する以前から予測を確認する為に
　HearschelのCO回転遷移の観測を利用した

・原始星が付随しないところでMHD乱流による散逸で予測されるショックの証拠を発見

・この領域で乱流の散逸のタイムスケールは横断時間と近い

・かなり密度が高い(10^3.5 cm^-3)の物質で一般的な分子雲よりも強い磁場(24uG)
　での乱流散逸のモデル予想と良く一致した。

TABLE 1
Source List

Source	Cloud	Dist	RA (J2000)	Dec
L1455-IRS3	Per	250	03h28m00.4s	+30d08m01.3s
IRAS 03301+3111	Per	250	03h33m12.8s	+31d21m24.2s
L1551-IRS5	Tau	140	04h31m34.1s	+18d08m04.9s
TMR 1	Tau	140	04h39m13.9s	+25d53m20.6s
TMC 1A	Tau	140	04h39m35.0s	+25d41m45.5s
TMC 1	Tau	140	04h41m12.7s	+25d46m35.9s
L1157	Core	325	20h39m06.3s	+68d02m16.0s
Isolated MC	Tau	140	04h39m53.0s	+25d45m00.0s

NOTE. — List of protostellar sources and the isolated molecular cloud position used in this sample, sorted by RA. Distances are measured in parsecs.

20. "Smoothed particle magnetohydrodynamic simulations of protostellar outflows with mis- aligned magnetic field and rotation axes"
Benjamin T. Lewis, Matthew R. Bate, and Daniel J. Price
Accepted by MNRAS   http://arxiv.org/pdf/1504.08322v1

ABSTRACT
We have developed a modified form of the equations of smoothed particle magnetohydrodynamics which are stable in the presence of very steep density gradients. Using this formalism, we have performed simulations of the collapse of magnetised molecular cloud cores to form protostars and drive outflows. Our stable formalism allows for smaller sink particles (< 5 AU) than used previously and the investigation of the effect of varying the angle, ϑ, between the initial field axis and the rotation axis. The nature of the outflows depends strongly on this angle: jet-like outflows are not produced at all when $\vartheta > 30°$, and a collimated outflow is not sustained when $\vartheta > 10°$. No substantial outflows of any kind are produced when $\vartheta > 60°$. This may place constraints on the geometry of the magnetic field in molecular clouds where bipolar outflows are seen.

Key words: accretion, accretion discs – MHD – stars: formation – stars: winds, outflows.

・急激な密度の勾配があるときに安定な smoothed particle magnetohydrodynamics (SPMHD)を改良した方程式を作った

・磁場がある分子雲ガスの収縮 (原始星形成、アウトフロー駆動)をシミュレーションした
・新しい方程式は、以前よりも小さなsink particleが可能で、初期の場の軸と回転軸の間の変化角θの効果を調べることが出来る。

・アウトフローはこの角度に強く依存する；jetのようなアウトフローはθ>30degの時には作られない、そしてcollimated outflowはθ>10degで維持されない。θ>60degでアウトフローは作られない。

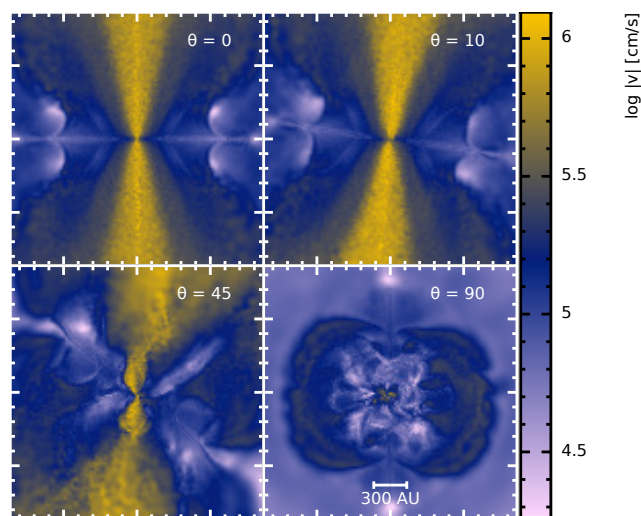・これはbipolar outflowが見えている場所での分子雲での磁場の方向に制約を課すことができると思われる。

Figure 11. Cross-sections of $|\mathbf{v}|$ at T = 27870 yrs (i.e. late enough that the magnetic effects seen in fig. 8 will have been able to disrupt the outflow). The two upper plots show the strongly collimated outflows seen for low values of ϑ whilst the $\vartheta = 45$ and 90° plots show the more complicated, diffuse outflows which at steeper angles essentially cease altogether.